JPn Neuroscience

The Journal of Physiology

J Physiol 594.10 (2016) pp 2661–2679

Optogenetic and pharmacological evidence that somatostatin-GABA neurons are important regulators of parasympathetic outflow to the stomach

Amanda E. Lewin, Stefano Vicini, Janell Richardson, Kenneth L. Dretchen, Richard A. Gillis and Niaz Sahibzada

Department of Pharmacology and Physiology, Georgetown University Medical Center, Washington, DC, USA

Key points

- The dorsal motor nucleus of the vagus (DMV) in the brainstem consists primarily of vagal preganglionic neurons that innervate postganglionic neurons of the upper gastrointestinal tract.
- The activity of the vagal preganglionic neurons is predominantly regulated by GABAergic transmission in the DMV.
- The present findings indicate that the overwhelming GABAergic drive present at the DMV is primarily from somatostatin positive GABA (Sst-GABA) DMV neurons.
- Activation of both melanocortin and μ-opioid receptors at the DMV inhibits Sst-GABA DMV neurons.
- Sst-GABA DMV neurons may serve as integrative targets for modulating vagal output activity to the stomach.

Abstract We have previously shown that local GABA signalling in the brainstem is an important determinant of vagally-mediated gastric activity. However, the neural identity of this GABA source is currently unknown. To determine this, we focused on the somatostatin positive GABA (Sst-GABA) interneuron in the dorsal motor nucleus of the vagus (DMV), a nucleus that is intimately involved in regulating gastric activity. Also of particular interest was the effect of melanocortin and μ-opioid agonists on neural activity of Sst-GABA DMV neurons because their *in vivo* administration in the DMV mimics GABA blockade in the nucleus. Experiments were conducted in brain slice preparation of transgenic adult Sst-IRES-Cre mice expressing tdTomato fluorescence, channelrhodopsin-2, archaerhodopsin or GCaMP3. Electrophysiological recordings were obtained from Sst-GABA DMV neurons or DiI labelled gastric-antrum projecting DMV neurons. Our results show that optogenetic stimulation of Sst-GABA neurons results in a robust inhibition of action potentials of labelled premotor DMV neurons to the gastric-antrum through an increase in inhibitory post-synaptic currents. The activity of the Sst-GABA neurons in the DMV is inhibited by both melanocortin and μ-opioid agonists. These agonists counteract the pronounced inhibitory effect of Sst-GABA neurons on vagal pre-motor neurons in the DMV that control gastric motility. These observations demonstrate that Sst-GABA neurons in the brainstem are crucial for regulating the activity of gastric output neurons in the DMV. Additionally, they suggest that these neurons serve as targets for converging CNS signals to regulate parasympathetic gastric function.

(Resubmitted 21 December 2015; accepted after revision 29 February 2016; first published online 9 March 2016)
Corresponding author N. Sahibzada: Department of Pharmacology & Physiology, Georgetown University Medical Center, Washington, DC 20057, USA. Email: sahibzan@georgetown.edu

DOI: 10.1113/JP272069

Abbreviations α-MSH, α-melanocortin stimulating hormone; aCSF, artificial cerebrospinal fluid; ArchT, archaerhodopsin; ChR2, channelrhodopsin; Cyppa, *N*-Cyclohexyl-*N*-[2-(3,5-dimethyl-pyrazol-1-yl)-6-methyl-4-pyrimidinamine; DAMGO, D-Ala^2,*N*-MePhe^4,Gly-ol]-enkephalin; DMV, dorsal motor nucleus of the vagus; EGFP, enhanced green fluorescent protein; GABAzine, 4-[6-imino-3-(4-methoxyphenyl)pyridazin-1-yl] butanoic acid hydrobromide; GIN, GFP expressing inhibitory neuron; IR, immunoreactivity; MC4R, melanocortin 4 receptor; MOR, μ-opioid receptor; NTS, nucleus tractus solitarius; PBS, phosphate-buffered saline; PRV, pseudorabies virus; sEPSC, spontaneous EPSC; sIPSC, spontaneous IPSC; sPSC, spontaneous postsynaptic current; Sst, somatostatin; THIQ, *N*-[(3R)-1,2,3,4-tetrahydroisoquinolinium-3-ylcarbonyl]-(1R)-1-(4-chlorobenzyl)-2-[4-cyclohexyl-4-(1H-1,2,4-triazol-1ylmethyl)piperidin-1-yl]-2-oxoethylamine.

Introduction

Over the years, a central question of great interest has been how activity in the reflex circuits of the brain controlling gastric function are regulated in response to both central and peripheral demands. A number of studies have highlighted the role of local GABA signalling as being paramount to mediating this function (Travagli *et al.* 1991; Smith *et al.* 1998; Glatzer *et al.* 2003; Davis *et al.* 2004; Bailey *et al.* 2008; Herman *et al.* 2009). To date, despite considerable evidence of the importance of local GABA in controlling gastric vagal circuitry, little is known about the identity and function of the neurons that underlie it. To address this question, we specifically focused on the contribution of local GABA in the nucleus that forms the efferent arm of the vagal circuitry that controls motility, namely the dorsal motor nucleus of the vagus (DMV) (Gillis *et al.* 1989; Rogers *et al.* 1996; Ferreira *et al.* 2002; Cruz *et al.* 2007; Richardson *et al.* 2013).

The DMV contains topographically arranged preganglionic neurons that project to distinct regions of the stomach (Pagani *et al.* 1985; Shapiro & Miselis, 1985; Pearson *et al.* 2007, 2011). Interspersed with these are small neurons (Jarvinen & Powley, 1999; Gao *et al.* 2009), some of which are green flourescent protein (GFP)-expressing inhibitory neurons (GIN) (Gao *et al.* 2009). In the brainstem, GIN neurons, as in the hippocampus and cortex (Oliva *et al.* 2000; Taniguchi *et al.* 2011), have been reported to express somatostatin and to have electrophysiological profiles (Wang & Bradley, 2010) functionally similar to the somatostatin positive GABAergic interneurons (Sst-GABA) that are present in other areas of the brain (Oliva *et al.* 2000; Halabisky *et al.* 2006; Ma *et al.* 2006; Fanselow *et al.* 2008; Taniguchi *et al.* 2011).

Because Sst-GABA have been shown to distinctly shape network dynamics in other areas (Fanselow *et al.* 2008; Fanselow & Connors, 2010; Gentet *et al.* 2012; Royer *et al.* 2012), they were the logical interneuron population to begin to decipher the contribution of local GABA signalling at the DMV. Of particular interest to us was the effect of melanocortin-4 receptor (MC4R) and μ-opioid (MOR) agonists on these neurons because their administration in the DMV increases vagally-mediated gastric activity (Herman *et al.* 2010; Richardson *et al.* 2013), which is an effect that resembles the blockade of local GABA within the nucleus (Sivarao *et al.* 1998; Ferreira *et al.* 2002; Herman *et al.* 2009). To accomplish this, we used transgenic Sst-IRES-Cre mice (Taniguchi *et al.* 2011) expressing either tdTomato, channelrhodopsin-2 (ChR2), ArchT-EGFP or GCaMP3 to: (1) determine whether optogenetic stimulation or inhibition of Sst-GABA neurons influences the activity of preganglionic motor neurons to the gastric-antrum; (2) establish that MC4R and MOR agonists inhibit neuronal activity of Sst-GABA neurons in the DMV; and (3) demonstrate that inhibition of vagal output activity as a result of Sst-GABA neuron stimulation can be prevented by pretreatment with MC4R or MOR agonists. In the present study, we report that optogenetic activation of Sst-GABA neurons inhibit the activity of identified DMV neurons projecting to the antral region of the stomach. This inhibition is prevented by pretreatment with MC4R or MOR agonists because exposure to these agonists blocks the activity of Sst-GABA neurons in the DMV. These observations demonstrate that inhibitory signalling in the DMV robustly controls vagal outflow to the stomach, leading us to propose that Sst-GABA neurons in the DMV are important integrative targets of upstream neurotransmitter systems mediating CNS control of gastric function.

Methods

Slice preparation, pharmacology and electrophysiology

The transgenic mice examined in the present study, for genetic identification of Sst-GABA DMV neurons and acute slice preparation, have been described previously (Luo *et al.* 2013; Partridge *et al.* 2014). All 'reporter' strains, as described within the relevant parts of the methods, are driven by Sst-Cre; *rosa26*-tdTom (Sst$^{tm2.1\ (cre)\ Zjh}$; Jackson Laboratory Strain 013044; The Jackson Laboratory, Bar Harbor, ME US) (Taniguchi *et al.* 2011)); channelrhodopsin-2 (CHR2-tdTomato; 'Ai27D'; Jackson Laboratory Stock no. 012567; The Jackson Laboratory), archaerhodopsin-3/enhanced green fluorescent protein (EGFP) 'reporter' (ArchT-EGFP; 'Ai40D'; Jackson Laboratory Stock no. 021188; The

Jackson Laboratory) and GCaMP3 'reporter' ('Ai38'; Jackson Laboratory Stock no. 014538; The Jackson Laboratory).

Ethical approval. Mice of either sex were killed by rapid decapitation in accordance with the National Institutes of Health (Bethesda, MD, USA) guidelines, UK regulations for ethical use of animals in research (Drummond, 2009) and with the approval of the Georgetown University Animal Care and Use Committee. In studies of electrophysiology recordings from Sst-GABA DMV neurons, brainstem slices were obtained from transgenic Sst-IRES-Cre mice expressing tdTomato red fluorescence (postnatal day 17–21). To record from identified gastric-antrum projecting DMV neurons, the cell viable monosynaptic tracer DiI was applied to the gastric-antrum of transgenic mice expressing CHR2-tdTomato or ArchT-EGFP (postnatal day 17–21) as described previously (Sahibzada *et al.* 2002). To allow for sufficient time for retrograde uptake of DiI in the gastric-antrum projecting DMV neurons, animals were allowed to recover for 7–10 days after surgery.

As previously described by us (Richardson *et al.* 2013), brains were quickly removed and placed in ice-cold oxygenated 'cutting' solution (95% O_2 + 5% CO_2; 4°C; pH 7.4; 296 mOsm l^{-1}) containing (in mM): 200 sucrose, 0.75 K-gluconate, 26 $NaHCO_3$, 1.25 KH_2PO_4, 0.5 $CaCl_2$, 7 $MgCl_2$, 5 glucose, 5 Hepes and 3 myo-inositol. Coronal brain sections (250 μm) containing the brainstem nuclei of the nucleus tractus solitarius (NTS) and DMV were cut using a vibratome (VT1000S; Leica Microsystems, Wetzlar, Germany) and incubated at 37°C for 30 min in oxygenated artificial cerebrospinal fluid (aCSF) (pH 7.4; 296 mOsm) with the composition (in mM): 121 NaCl, 2.5 KCl, 26 $NaHCO_3$, 1.25 NaH_2PO_4, 2 $CaCl_2$, 1 $MgCl_2$, 5 Hepes and 2.5 glucose. They were then allowed to equilibrate for an additional 30 min at room temperature (21°C). Subsequently, the slices were transferred to a recording chamber (500 μl volume) attached to the stage of a microscope (E600-FN; Nikon, Tokyo, Japan). There, they were continuously perfused with oxygenated aCSF [note that the aCSF with low Ca^{2+} comprised (in mM): 123 NaCl, 2.5 KCl, 26 $NaHCO_3$, 1.25 NaH_2PO_4, 0.2 $CaCl_2$, 9.10 $MgCl_2$, 5 Hepes and 2.5 glucose. The solution was corrected for osmolarity, which was typically 296 mOsm l^{-1}].

Neurons were identified visually by infrared-differential interference contrast or episcopic fluorescence optics and a CCD camera (Dage S-75, Dage-MTI, Michigan City, IN, USA). A 60× water immersion objective was used for identifying and approaching neurons. Recordings were made with patch electrodes (5–6 MΩ; Warner Instruments, Hamden, CT, USA) with internal pipette solution (pH 7.2; 285 mOsm l^{-1}) that comprised (in mM): 145 K-gluconate, 5 EGTA, 5 MgCl2, 10 Hepes, 5 ATP·Na and 0.2 GT- P.Na. In studies in which IPSCs were specifically studied, 145 mM KCl was substituted for potassium gluconate in the pipette solution. Cell-attached (loose seal <40 MΩ), whole-cell voltage clamp (V_{hold} = −60 mV or −30 mV) or current clamp recordings were performed using a MultiClamp 700B amplifier (Molecular Devices, Sunnyvale, CA, USA) (note that the action potential firing frequency was not significantly different in parallel cell-attached recordings with aCSF pipette solution). Input and access resistances were monitored by a 5 mV hyperpolarization pulse; series resistance was typically <10 MΩ and was not compensated. Resting membrane potentials were corrected for liquid junction potential, which, for the intracellular solution K-gluconate, was −15 mV and, for the KCl, was −3 mV. Signals were low-pass filtered at 2 KHz and acquired with a Digidata 1440A (Molecular Devices).

Optogenetic stimulation

Coronal brainstem slices were obtained from mice with a Cre-dependent channelrhodopsin2-tdTomato 'reporter' (CHR2-tdTomato; 'Ai27D'; Jackson Laboratory Stock no. 012567; The Jackson Laboratory) or archaerhodopsin-3/EGFP 'reporter' (ArchT-EGFP; 'Ai40D'; Jackson Laboratory Stock no. 021188; The Jackson Laboratory) that had DiI (cell viable monosynaptic retrograde tracer) applied to the antrum region of their stomachs as described previously (Richardson *et al.* 2013). Light stimulation was accomplished in two ways: (1) local stimulation (1 s duration) via a 60× water objective utilizing filter cubes (CHR2-tdTomato, 450–490 nM; ArchT-EGFP 510–560 nM) of the microscope or (2) non-local stimulation (1 s duration) using a laser-coupled fibre optic cable attached to a 'fibre cannula', which was placed directly above the NTS-DMV brainstem area (Lasers wavelengths: blue light ∼473 nM, 1.20 μW and green light ∼532 nM, 1.36 μW; Shanghai Laser & Optics Century Co., Shanghai, China; optic fibre/cable, part no. BFL37-200; Thorlabs Inc., Newton, NJ, USA). The diameter of the area exposed to optogenetic stimulation under the 60× objective was <100 μm, whereas the extent of the blue light from the laser-coupled fibre cannula encompassed the whole NTS-DMV brainstem area.

Intracellular calcium measurements

Coronal slices from Cre-dependent GCaMP3 'reporter ('Ai38'; Jackson Laboratory Stock no. 014538; The Jackson Laboratory) were acutely prepared from animals that were inoculated with the polysynaptic retrograde tracer pseudorabies virus (PRV-152EGFP) in the antrum of

the stomach as described previously (Niedringhaus *et al.* 2008) (PRV-152EGFP was a gift from Dr Lynn Enquist, Princeton University Centre for Neuroanatomy with Neurotropic Viruses, NIH grant number P40RR018604). Imaging experiments were performed as described previously (Partridge *et al.* 2014). Briefly, imaging was performed by integrating a patch clamp set-up with laser scanning confocal hardware (CLS; Thor Imaging Systems Division, Sterling, VA, USA) mounted on an Eclipse FN1 upright microscope (Nikon) equipped with a 60× water immersion lens or a 20× dry lens. Time series images were acquired at a rate of ∼2.4 Hz at a resolution of 512 × 512 pixels following light detection by photomultiplier tubes averaged over six frames. For chemical stimulation, local application of a solution with a high KCl concentration (40 mM) was employed via the 'Y-tube method'. For electrical stimulation, square-wave pulses (100–300 μA, pulse width 50 μs, 0.1 Hz) were delivered by placement of a bipolar stimulating electrode near the region being imaged. All subsequent drug application was applied via the 'Y-tube method'.

Immunolocalization

Brainstem sections were obtained from ∼3 week postnatal day transgenic Sst-IRES-Cre mice expressing tdTomato red fluorescence. Following anaesthesia with isoflurane, mice were initially perfused transcardially with phosphate-buffered saline (PBS; 0.1 M; pH 7.3), which was then followed by 4% buffered paraformaldehyde. The brains were removed and stored overnight in 4% paraformaldehyde. Free-floating coronal brainstem sections (50 μm) were obtained using a vibratome (VT1000S; Leica Microsystems). Sections were blocked with 4% donkey serum in PBS for 1 h at room temperature and washed three times for 10 min each in PBS containing 0.1% Triton-X100. They were then incubated overnight (minimum 12 h; 4 °C) with a primary somatostatin antibody (polyclonal rabbit; dilution 1:400; ImmunoStar Inc., Hudson, WI, USA) that was diluted in PBS/Triton-X100/1% BSA. Following this treatment, the brainstem sections were washed again three times for 10 min each in PBS/Triton-X100 and incubated further (2–4 h) at room temperature with a secondary anti-rabbit antibody conjugated to Alexa-488 (dilution 1:500; Life Technologies, Grand Island, NY, USA), which was constituted in PBS/Triton-X100/BSA. At the end of the incubation, the brainstem slices were again washed three times for 10 min each with PBS/Triton-X100. To obtain confocal images, a brainstem slice was transferred into the viewing chamber of a confocal microscope (see Ca^{2+} imaging experiments). Acquired Z-stack images (1 μm) were processed with ImageJ (National Institutes of Health).

Drugs

Stock solutions of the following drugs were prepared in water and were obtained from: α-melanocyte-stimulating hormone (α-MSH, Ac-Ser-Tyr-Ser-Met-Glu-His-Phe-Arg-Trp-Gly-Lys-Pro-Val-NH2) (Phoenix Pharmaceuticals, Burlingham, CA, USA); *N*-[(3R)-1,2,3,4-tetrahydroisoquinolinium-3-ylcarbonyl]-(1R)-1-(4-chlorobenzyl)-2-[4-cyclohexyl-4-(1H-1,2,4-triazol-1ylmethyl)piperidin-1-yl]-2-oxoethylamine (THIQ), 4-[6-imino-3-(4-methoxyphenyl)pyridazin-1-yl] butanoic acid hydrobromide (GABAzine) and *N*-cyclohexyl-*N*-[2-(3,5-dimethyl-pyrazol-1-yl)-6-methyl-4-pyrimidinamine (CyPPA) (R&D Systems, Minneapolis, MN, USA); TTX (Abcam Inc., Cambridge, MA); and D-Ala^2,*N*-MePhe^4, Gly-ol]-enkephalin (DAMGO) (Sigma-Aldrich, St Louis, MO, USA). Drug-containing stock solutions were diluted to desired concentrations in either aCSF or low calcium aCSF (adjusted for osmolarity, which was typically 296 mOsm l^{-1}). All drugs were applied via bath application.

Data analysis

Electrophysiological data were analysed offline using pClamp, version 10 (Molecular Devices) and MiniAnalysis (Synaptosoft Inc., Fort Lee, NJ, USA). To measure the rate of action potentials, data were acquired from neurons that had a stable baseline membrane potential and amplitude of −60 mV.

To analyse postsynaptic currents, a semi-automated threshold-based software was employed (Mini Analysis; Synaptosoft Inc.) and the currents confirmed visually based on: (1) rise time; (2) exponential decay; and (3) threshold (five to 10 times the baseline noise depending on the voltage clamp (V_{hold} = −60 mV or −30 mV)) and the internal pipette solution (K-gluconate or KCl). The control and treatment data were acquired from two consecutive 500 ms segments. In studies where optogenetic stimulation was employed to activate Sst-GABA-ChR2 DMV neurons when recording from gastric-antrum projection DMV neurons, the voltage clamp was set at −30 mV. This was also the case when recordings were made from Sst-GABA DMV neurons expressing tdTomato fluorescence. This procedure allowed us to separate IPSCs and EPSCs, which were displayed as upward deflections (outward currents) and downward deflections (inward currents), respectively. Both IPSCs and EPSCs were measured together because there was minimal, if any, overlap between the two types of currents. Moreover, it enabled us to clearly visualize a one-to-one correlation between the onset of the optogenetic stimulation and its effect on the identity of the postsynaptic current (i.e. IPSC or EPSC).

Statistical analysis

Statistical analyses were performed using Prism (GraphPad, La Jolla, CA, USA) or Excel (Microsoft Corp, Redmond, WA, USA). All data were normalized and the results are expressed as the mean ± SEM. A Kolmogorov–Smirnov test was used to detect significant variation in postsynaptic currents within cells in response to a treatment condition, whereas group differences to assess significant differences between control and treatment conditions were determined using a paired Student's *t* test or one-way ANOVA. Treatment interactions were assessed by Tukey's *post hoc* multiple comparisons test. $P < 0.05$ was considered statistically significant.

Results

Transgenic targeting of Sst-GABA neurons in the DMV

In addition to the role of Sst-GABA neurons as important regulators of network dynamics in various regions of the brain (Fanselow *et al.* 2008; Fanselow & Connors, 2010; Royer *et al.* 2012), their prominent distribution as visualized by tdTomato red fluorescence protein in the brainstem, including the DMV (Fig. 1*A* and *B*), further justified their suitability as good candidates for discerning the contribution of local GABA towards regulation of vagal outflow to the stomach. When employing transgenic Sst-IRES-Cre mice expressing different constructs to do this, it was imperative that we first confirm the identity of the neurons that we planned to activate or record. The reason for this stems from reports that Sst–IRES-Cre-mediated recombination is not solely restricted to Sst-GABA neurons. Instead, for example, in the cortex, at least 6–10% of neurons are fast spiking parvalbumin neurons that are 'miss-expressed' by a Cre-dependent reporter (Hu *et al.* 2013). To ensure that the neurons we were targeting in the DMV had our desired genetic labelling, we confirmed their identity using electrophysiological cell-typing protocol and immunohistochemistry.

Depolarizing current injection into the Sst-GABA neurons in the DMV of Sst-IRES-Cre mice expressing tdTomato red fluorescence ($n = 9$) (Fig. 1*C*) displayed electrophysiological properties similar to a subset of these neurons reported in other areas of the brain (Oliva *et al.* 2000; Ma *et al.* 2006; Luo *et al.* 2013). These neurons showed almost no change in spike frequency adaptation (accommodation) in response to depolarizing current (Fig. 1*C*); their firing pattern resembling those, for example designated as classical non-accommodating interneurons in the cortex (Markram *et al.* 2004). However, unlike other areas (Oliva *et al.* 2000; Ma *et al.* 2006; Wang & Bradley, 2010), Sst-GABA neurons in the DMV did not exhibit any noticeable depolarization 'sag' when exposed to hyperpolarizing current steps, which is indicative of the presence of hyperpolarization-activated non-selective cation channels (Robinson & Siegelbaum, 2003).

In addition to the Sst-GABA DMV neurons displaying an electrophysiological profile similar to those in other areas of the brain, histochemical processing of the brainstem sections revealed that ∼90% of DMV neurons ($n = 78$) that could be unequivocally identified expressing the Cre-dependent reporter (tdTomato) displayed immunoreactivity (IR) for the somatostatin-28 antibody (Fig. 1*D–I*), which appeared to be restricted to the perikaryal cytoplasm. Somatostatin-IR was also present in the surrounding neuropil as was evident from the labelled fibres and puncta (Fig. 1*D–I*) (no IR for the somatostatin-28 antibody was observed in any non-tdTomato expressing neurons).

To establish that the identified Sst-GABA DMV neurons are part of the gastric-antrum circuit, we injected PRV-152 EGFP into the gastric-antrum of Sst-IRES-Cre mice expressing tdTomato red fluorescence ($n = 8$). In all mice, after a 48–72 h survival period, PRV transynaptically labelled Sst-GABA neurons in the DMV (Fig. 1*L–M*). This confirmed that the vagal circuit controlling the gastric-antrum does indeed incorporate the genetically identified Sst-GABA neurons in the DMV.

Optogenetic stimulation of Sst-GABA DMV neurons affects neural activity of pre-motor gastric-antrum projecting DMV neurons

To understand the extent and manner by which local GABA signalling (specifically that of Sst-GABA neural origin) in the DMV influences vagal output to the stomach, we employed optogenetic stimulation or inhibition in transgenic mice with ChR2 or ArchT expression driven by Sst-IRES-Cre. Recordings were made from visually identified gastric-antrum-projecting neurons in the DMV that were retrogradedly labelled by the cell viable fluorescent tracer DiI (Richardson *et al.* 2013). Our reason for focusing on DMV neurons projecting to the gastric-antrum was two-fold. First, the gastric-antrum is an important source of gastric motility (el-Sharkawy *et al.* 1978; Gillis *et al.* 1989; Ludtke *et al.* 1991; Rogers *et al.* 1996). Second, GABAergic blockade in the DMV specifically influences gastric motility (Herman *et al.* 2010; Richardson *et al.* 2013). To ensure that Sst-GABA DMV neurons were being optogenetically activated or inhibited, in some experiments, recordings were directly made from these neurons and their responses assessed to light exposure. Figure 2*A* shows the extent of the area (<100 μm diameter) stimulated by episcopic light stimulation using a 60× water objective.

Optogenetic stimulation of Sst-GABA-ChR2 neurons inhibits action potential frequency of pre-motor antrum-projecting DMV neurons. When exposed to blue light (λ = 450–490 nm), Sst-GABA-ChR2 neurons in the DMV increased their action potentials in both the cell attached (n = 5/5; t_4 = 2.8, $P < 0.05$) and current clamp configuration (n = 7/7; t_6 = 3.7, $P < 0.01$) (Fig. 2*B*–*E*). Conversely, light stimulation of Sst-GABA-ChR2 neurons suppressed action potentials in 78% of DMV gastric-antrum projecting neurons from a baseline frequency of 1.68 ± 0.27 Hz to that of 0.15 ± 0.04 Hz (n = 14/18; t_{13} = 4.2, $P < 0.0005$) (Fig. 2*F* and *G*). This response was repeatable without any significant attenuation in the light-induced inhibitory events (Fig. 2*H*). In a few DMV output neurons (n = 4/18) (Fig. 2*N*), blue light was ineffective in that it neither decreased, nor increased the rate of action potentials firing in these neurons.

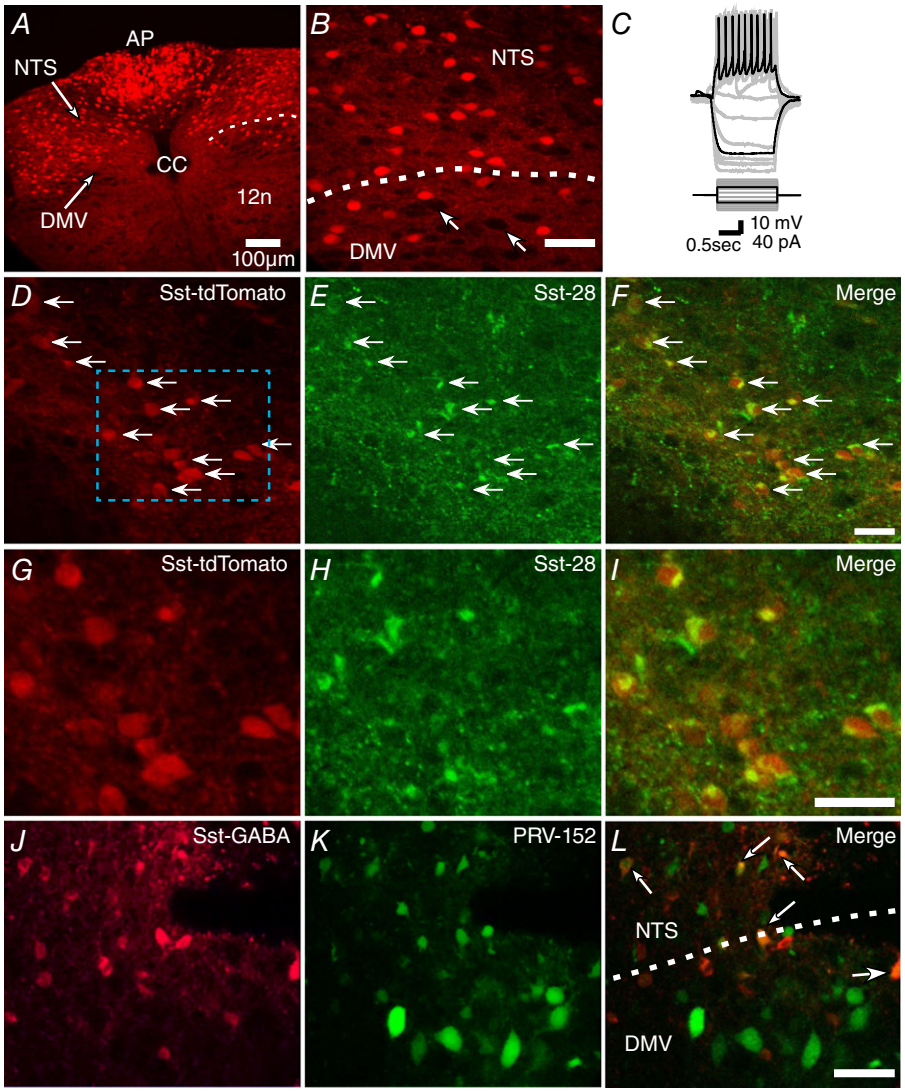

Figure 1. Distribution of Sst-GABA neurons in the dorsal vagal complex (DVC)
A, photomicrograph showing the distribution of Sst-GABA neurons expressing tdTomato red fluorescence in the DVC. *B*, enlarged image of the area around the stippled line in (*A*) showing Sst-GABA neurons in the NTS and DMV. [Note: arrows depict large unlabeled DMV output neurons.] *C*, current clamp recording showing the characteristic action potential profile of a Sst-GABA neuron in the DMV in response to current steps. *D*–*F*, representative images of neurons in the DMV showing tdTomato expression in Sst-GABA neurons (*D*) and IR for Sst-28 antibody (*E*) and their superimposition (*F*). *G*–*I*, higher magnification images of the stippled area in (*D*) showing co-localization of genetically defined Sst-GABA (*G*) and Sst-28 immunoreactive (*H*) neurons. *J*–*M*, Sst-GABA (*J*) and PRV-152 labelled neurons (*L*) in the DMV and NTS that were trans-neuronally dual-labelled (*M*, arrows) from the gastric-antrum. 12n, hypoglossal; AP, area postrema; CC, central canal; DMV, dorsal motor nucleus of the vagus; NTS, nucleus tractus solitarius. Scale bars = 50 μm.

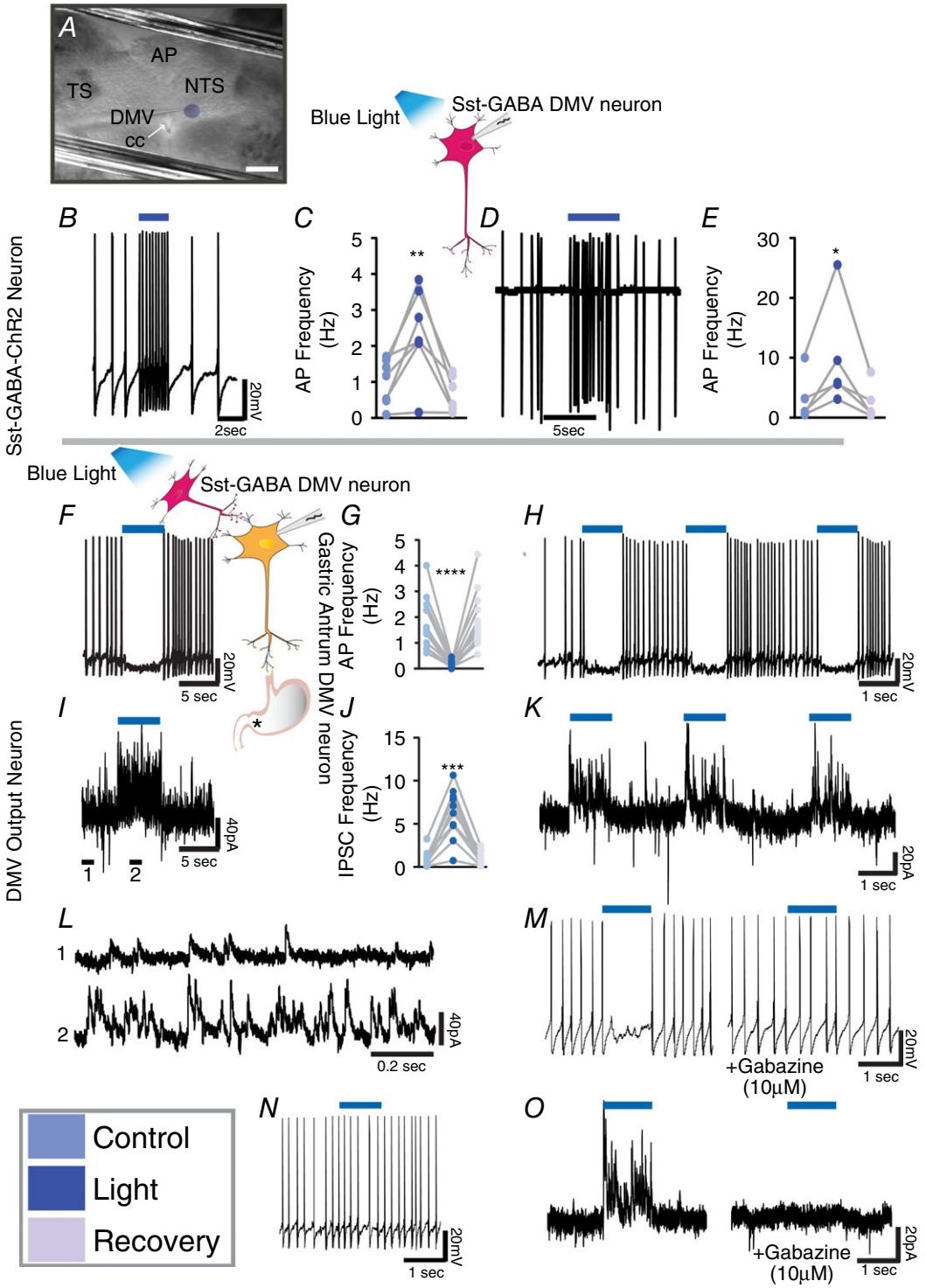

Figure 2. Optogenetic stimulation of Sst-GABA-ChR2 neurons in the DMV inhibits vagal output neurons in the nucleus that innervate the gastric-antrum
A, photomicrograph showing a recording electrode in the DMV and the extent of the area (purple circle) illuminated by optogenetic stimulation. Scale bar = 200 μm. *B*, direct light stimulation (blue bar) of a Sst-GABA-ChR2 neuron increases its action potential frequency. *C*, stimulatory effects of light on action potential frequency in Sst-GABA neurons during current clamp recording ($n = 7$; $^{**}P < 0.01$). *D* and *E*, a similar increase is seen in action potential

Activation of Sst-GABA-ChR2 neurons increase spontaneous IPSCs (sIPSCs) in pre-motor antrum-projecting DMV neurons. To identify the neurotransmitter responsible for the light-induced inhibition of DMV output neurons, each cell underwent exposure to blue light (λ 450–490 nm) in the voltage clamp mode (V_{hold} = −30 mV). In all cells studied (n = 11), light stimulation induced a distinct increase in the frequency and amplitude of IPSCs ($t_{10} = 4.6$, $P < 0.001$ and $t_6 = 3.7$, $P < 0.01$, respectively) (Fig. 2*I–L*). Stimulation of IPSCs coincided with the light-induced inhibitory effect on action potentials in DMV neurons (Fig. 2*F*, with the corresponding IPSCs shown in Fig. 2*I*). Moreover, both light-induced inhibition of action potentials and light-induced stimulation of IPSCs were abolished by the $GABA_A$ receptor antagonist, gabazine (10 μM) (Fig. 2*M* and *O*); hence, there was 0% change in either IPSCs or action potential frequency (n = 5) during light stimulation.

Optogenetic inhibition of Sst-GABA neurons affects the frequency of synaptic currents in pre-motor gastric-antrum projecting DMV neurons. To determine whether Sst-GABA neurons were a source of tonic inhibition on DMV output neurons, recordings were made from brainstem slices obtained from transgenic mice expressing the proton transporting opsin, ArchT selectively in Sst-GABA neurons. Light exposure (λ = ∼575 nm) silenced the action potentials of Sst-GABA-ArchT neurons in the DMV from a baseline frequency of 4.6 ± 2.1 Hz to a frequency of 0 Hz during light activation (n = 5, t_4 = 2.1, $P < 0.05$) (Fig. 3*A–C*). Recordings were then made from retrogradedly labelled DMV neurons. Optogenetic inhibition of Sst-GABA-ArchT neurons was accompanied by a significant decrease in spontaneous postsynaptic currents (sPSCs) in antrum projecting DMV neurons from a mean frequency of 5.6 ± 1.8 Hz to 1.8 ± 0.6 Hz (n = 4, $t_3 = 2.8$, $P < 0.05$) (Fig. 3*D* and *E*).

To determine whether Sst-GABA DMV neurons are themselves under tonic inhibition, they were exposed to bath application of low $[Ca^{2+}]_o$ (0.2 nM; n = 14) in the loose cell-attached mode. Exposure to low $[Ca^{2+}]_o$ increased the frequency of action potentials two-fold (from a baseline of 0.65 ± 0.26 Hz to 1.97 ± 0.41 Hz; $t_{13} = 5.12$, $P < 0.001$), which was attenuated by the SK channel positive modulator (CyppA 10 μM; from a baseline of 2.63 ± 0.74 Hz to 0.41 ± 0.22 Hz; $t_3 = 3.2$, $P < 0.05$).

These studies demonstrate that Sst-GABA neurons are important regulators of the parasympathetic pre-motor neurons that innervate the gastric-antrum. This regulation of vagal output activity occurs via a GABAergic pathway that is tonically active. Furthermore, the data indicate that the Sst-GABA neurons in the DMV are themselves under tonic inhibitory drive from as yet an unknown source.

Activation of melanocortin-4 receptors affects neural activity of Sst-GABA neurons in the DMV

Stimulation of MC4Rs in the DMV by the endogenous melanocortin agonist, α-MSH, increases gastric motility (Richardson *et al.* 2013) in a manner that resembles local GABA blockade (Sivarao *et al.* 1998) in the nucleus. To determine whether these effects could be mediated through inhibition of the tonically active Sst-GABA DMV neurons, we performed electrophysiology in brainstem slices of transgenic Sst-IRES-Cre mice (Taniguchi *et al.* 2011) expressing tdTomato red fluorescence. Because MC3Rs have not been reported to be present in the dorsal vagal complex that includes the NTS and DMV (Roselli-Rehfuss *et al.* 1993; Kistler-Heer *et al.* 1998; Iqbal *et al.* 2001), both our previous *in vivo* and present *in vitro* data are in reference to the activation of MC4Rs in these nuclei.

Melanocortin agonist inhibit action potential frequency. In the cell-attached mode (loose seal <40 MΩ), the effect of α-MSH (500 nM) was examined on the spontaneous action potential frequency of Sst-GABA neurons in the DMV. Bath application of α-MSH for 3–5 min significantly attenuated the mean neuronal firing rate from baseline by 77 ± 7% (n = 12; $t_{11} = 5.2$, $P < 0.001$; baseline, 2.11 ± 0.33 Hz; α-MSH, 0.50 ± 0.14 Hz) (Fig. 4*A* and *C*) in a reversible manner. Similarly, inhibition of action potential frequency was observed in the current clamp mode upon bath exposure to α-MSH (Fig. 4*B*). Exposure to α-MSH not only suppressed the action potentials in the Sst-GABA DMV neurons (n = 7; 99 ± 1% from baseline; $t_6 = 5.2$, $P < 0.01$; baseline, 3.73 ± 0.95 Hz; Mc4R agonist,

frequency of Sst-GABA neurons recorded in the cell-attached mode (n = 5; $^*P < 0.05$). *F*, representative current clamp recording showing light-induced (blue bar) inhibition of action potential firing in a DMV antrum projection neuron. *G*, inhibitory effects of Sst-GABA stimulation on action potential frequency of gastric-antrum projecting neurons (n = 14/18; $^{****}P < 0.005$). *H*, current clamp recording demonstrating the repeatability of light-induced inhibition in a DMV antrum projection neuron. *I*, voltage clamp recording (V_H = −30) from the cell in (*F*) showing that light stimulation (blue bar) is accompanied by an increase in IPSCs. *J*, light stimulation robustly increases sIPSCs in antrum projecting neurons (n = 11; $^{***}P < 0.001$), which is repeatable (*K*). *L*, expanded view of regions 1 and 2 in the tracing in (*I*), showing sIPSCs before (1, top) and during light stimulation of Sst-GABA neurons (2, bottom). *M*, the decrease in light-induced action potentials is prevented by pretreatment with gabazine. *N*, representative tracing of action potentials in a DMV antrum projection neuron that was unaffected by optogenetic stimulation. *O*, increase in IPSCs as a result of light stimulation is blocked by gabazine. Blue bar = light with λ of 450–490 nm.

0.03 ± 0.03 Hz) (Fig. 4*D*), but also hyperpolarized their membrane ($n = 8$; $t_7 = 4.6$, $P < 0.01$; baseline −40 ± 3 mV; MC4R −51 ± 3 mV) (Fig. 4*E*). In the presence of TTX (1 μM), α-MSH had no effect on membrane potential (Fig. 4*F*).

Melanocortin agonist differentially effects sPSCs. To discern the synaptic nature of the α-MSH-induced inhibition on neural activity of Sst-GABA DMV neurons, whole-cell recordings were obtained in brainstem slices from neurons that were voltage clamped at −30 mV. Bath application of α-MSH (500 nM) significantly increased the frequency of sIPSCs (Fig. 4*I*) by two-fold from an average baseline frequency of 0.44 ± 0.14 to 0.68 ± 0.17 ($t_{13} = 3.2$, $P < 0.01$) (Fig. 4*J*). This increase in sIPSC frequency was blocked by bath application of TTX (1 μM). In all cells studied, α-MSH did not affect the amplitude of sIPSCs or mIPSCs in the Sst-GABA DMV neurons (Fig. 4*K*).

By contrast to sIPSCs, α-MSH decreased the rate of spontaneous EPSCs (sEPSCs) from an average baseline of 1.38 ± 0.35 Hz to that of 0.98 ± 0.25 Hz (sEPSCs; $t_{14} = 2.7$, $P < 0.05$; Fig. 4*I* and *L*). Similar to sIPSCs, the amplitude of the excitatory currents was unaffected (Fig. 4*I* and *M*). The α-MSH-induced decrease in sEPSCs frequency was blocked by pretreatment with TTX (1 μM), thus establishing that they were action potential-dependent presynaptic events.

Activation of μ-opioid receptors (MOR) affects neural activity of Sst-GABA neurons in the DMV

Similar to melanocortin receptor stimulation, MOR activation also profoundly affects gastric motility that reflects inhibition of local GABA signalling in the dorsal vagal complex (Herman *et al.* 2010). In the DMV, as with α-MSH (Richardson *et al.* 2013), DAMGO increases gastric motility (Herman *et al.* 2010), which also resembles GABA blockade in the nucleus (Herman *et al.* 2010). To determine whether activation of MORs in the DMV mirrored the effects seen with MC4R activation, Sst-GABA

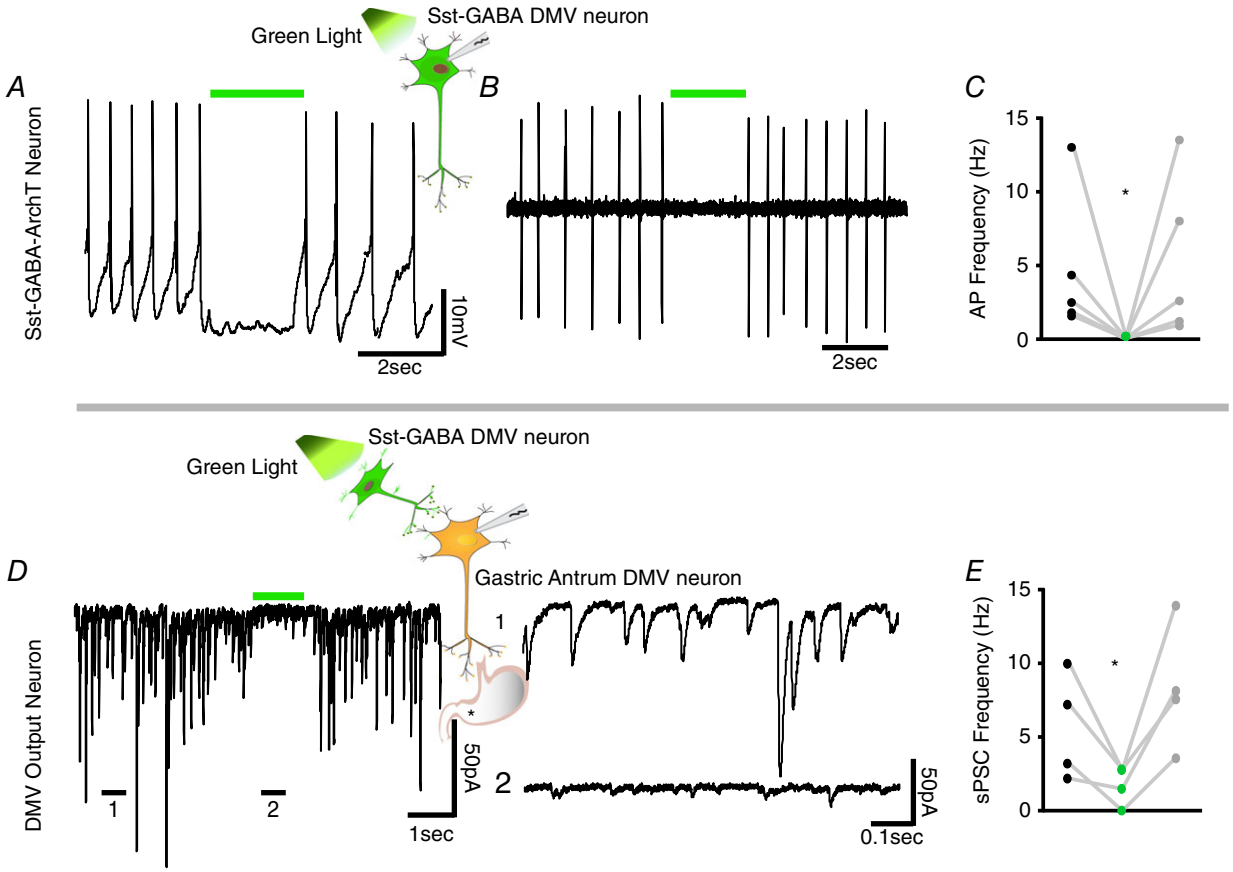

Figure 3. Optogenetic inhibition of Sst-GABA-ArchT neurons in the DMV reduces sPSCs in vagal output neurons that innervate the gastric-antrum
A and *B*, respective current clamp and loose cell attached recordings from a Sst-GABA-ArchT neuron in the DMV that demonstrates light-induced inhibition (green bar). *C*, light-induced inhibition of Sst-GABA neurons ($n = 5$; $^*P < 0.05$). *D*, left: exposure of Sst-GABA-ArchT neurons to light (green bar) inhibits IPSCs in antrum-projecting vagal neurons. *D*, right: expanded views of regions 1 and 2 depicted in (*D*, left). *E*, light-induced inhibition of postsynaptic current originating from Sst-GABA neurons ($n = 4$; $^*P < 0.05$). Green bar = light with λ of ~575 nm.

DMV neurons were exposed to bath application of DAMGO (1 μM).

MOR agonist, inhibits action potential frequency. In the loose cell attached mode, bath application of DAMGO blocked action potentials by 97 ± 2 % (t_9 = 3.2, $P < 0.01$; baseline, 2.93 ± 0.9; DAMGO, 0.14 ± 0.08) (Fig. 5*A* and *C*). In the current clamp mode, bath application of DAMGO robustly blocked the generation of action potentials (Fig. 5*B*). From an average frequency of 3.75 ± 1.04 Hz, exposure to DAMGO resulted in a 97 ± 3% decrease in frequency (0.63 ± 0.6 Hz; $t_8 = 2.8$, $P < 0.05$) (Fig. 5*D*). Additionally, DAMGO significantly hyperpolarized the membrane from a resting potential of −38 ± 3 mV to that of −50 ± 3 mV (t_{15} = 4.11, $P < 0.001$) (Fig. 5*B* and *E*). This was also evident after pretreatment with TTX (1 μM; n = 14, −39 ± 3 mV; DAMGO, −43 ± 3 mV; t_{13} = 3.03, $P < 0.01$) (Fig. 5*F*). The hyperpolarization was accompanied by a change in input resistance from a baseline of −13 ± 4 mV to that of 4 ± 6 mV (t_{15} = 4.49, $P < 0.001$) (Fig. 5*G* and *H*).

MOR stimulation differentially effects sPSCs. The decrease in neuronal activity caused by MOR activation was further assessed in terms of synaptic function as it relates to sPSCs. Unlike MC4Rs, activation of MORs by DAMGO was accompanied by a 88 ± 3% decrease in sIPSCs frequency ($t_{17} = 3.2$, $P < 0.01$; baseline, 1.13 ± 0.3; DAMGO, 0.16 ± 0.04) (Fig. 5*G* and *I*) and amplitude (control 18.25 ± 1.68 pA; DAMGO 12.54 ± 0.80 pA; $t_9 = 3.5$, $P < 0.01$) (Fig. 5*G* and *J*).

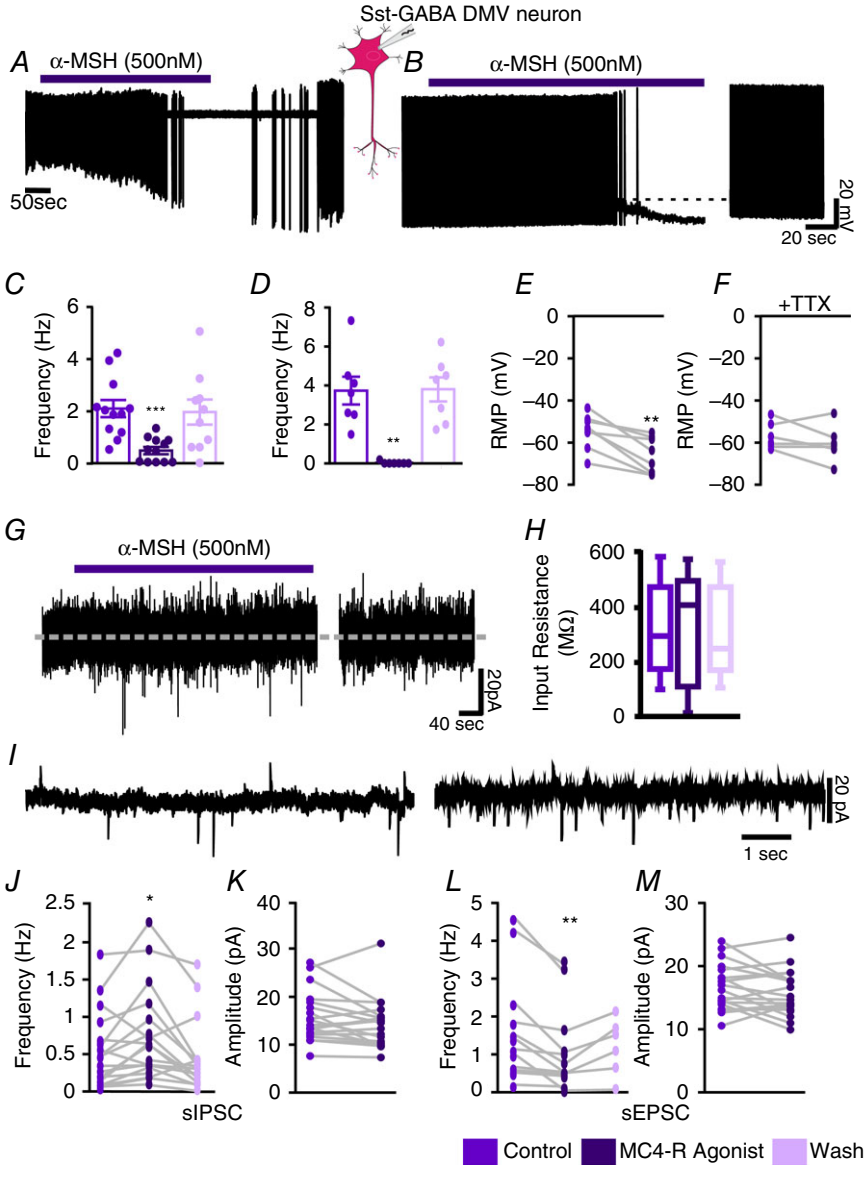

Figure 4. MC4R agonist inhibits Sst-GABA neurons in the DMV
A, representative loose cell-attached recording from a Sst-GABA neuron and its inhibition by α-MSH. *B*, representative current clamp recording from a Sst-GABA neuron in the absence and presence of α-MSH. *C* and *D*, summaries of the effects of α-MSH on action potential frequency in Sst-GABA neurons in the DMV in the cell-attached (n = 12; $^{***}P < 0.001$) and current clamp modes (n = 7; $^{**}P < 0.01$), respectively. *E* and *F*, summaries of the effects of α-MSH on resting membrane potential (RMP) in Sst-GABA neurons in the DMV (n = 8; $^{**}P < 0.01$) in the absence (*E*) and presence (*F*) of TTX (n = 6, $P > 0.05$). *G*, representative voltage clamp recording showing direct membrane current or input resistance (*H*) α-MSH. *I*, representative voltage clamp recording (V_H = −30 mV) showing sPSCs before (left) and during (right) exposure to α-MSH. *J*, α-MSH increases sIPSC frequency of Sst-GABA neurons in the DMV (n = 16; $^{**}P < 0.01$). *K*, sIPSC amplitude of Sst-GABA neurons in the DMV is unaffected by α-MSH (n = 18). *L*, α-MSH decreases the sEPSC frequency of Sst-GABA neurons in the DMV (n = 17; $^{**}P < 0.01$) but has no effect (*M*) on sEPSC amplitude (n = 19).

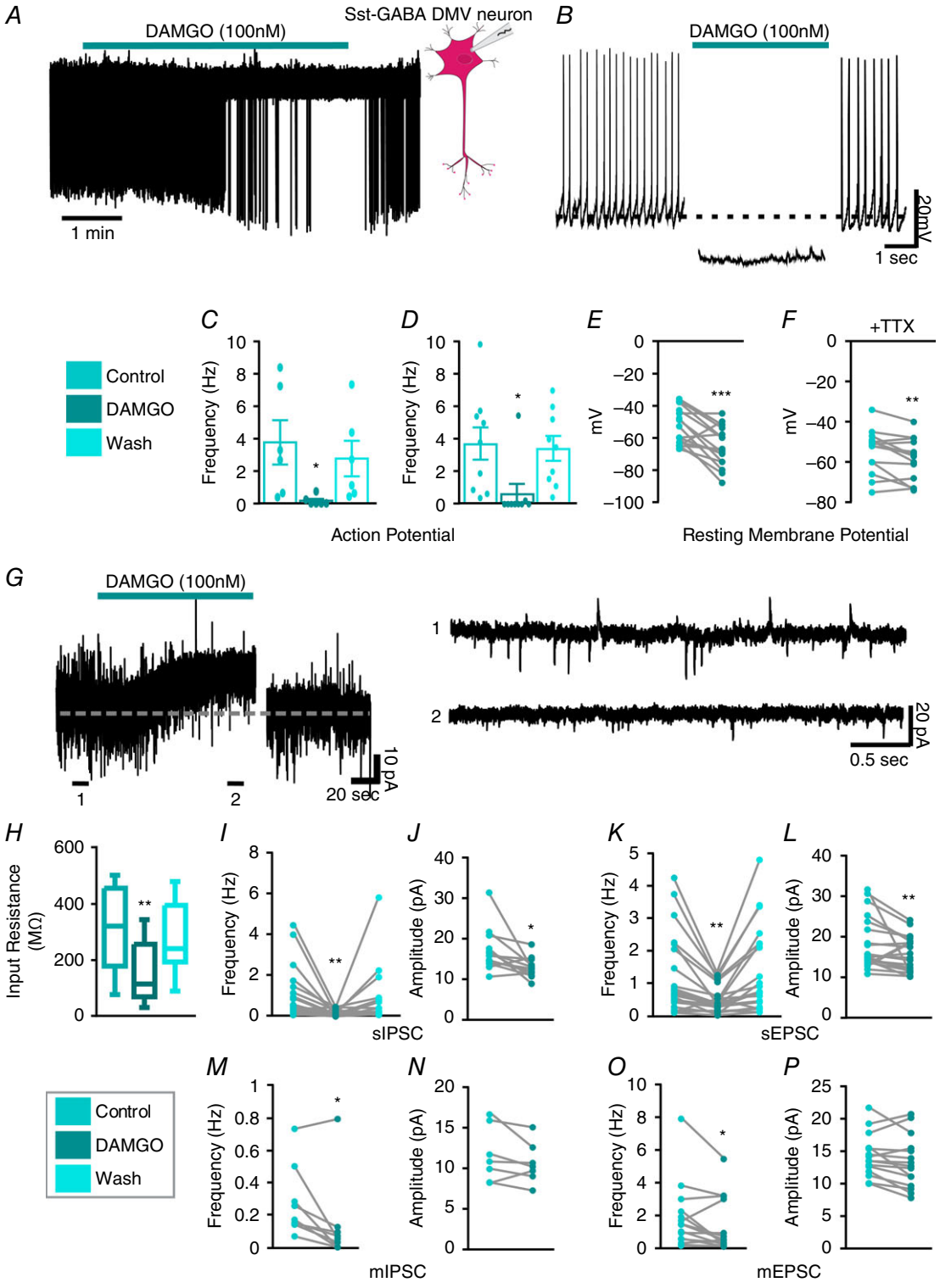

Figure 5. MOR agonist inhibits Sst-GABA neurons in the DMV
A, representative loose cell attached recording from a Sst-GABA neuron that is inhibited by the MOR agonist, DAMGO. *B*, representative current clamp recording from a Sst-GABA neuron illustrating the effect of DAMGO on its action potential firing and membrane potential. *C* and *D*, DAMGO inhibits action potential frequency in Sst-GABA neurons in the loose cell attached mode (*C*, $n = 10$; $^{**}P < 0.01$) and in current clamp mode (*D*, $n = 9$; $^{*}P < 0.05$). *E* and *F*, DAMGO decreases the resting membrane potential (RMP) of Sst-GABA neurons ($n = 16$; $^{****}P < 0.0005$) in the absence (*E*) and presence (*F*) of TTX ($n = 14$, $^{***}P < 0.001$).

Similar to sIPSCs, the frequency of sEPSCs was also attenuated on exposure to DAMGO but by 58 ± 5% (control 1.41 ± 0.20 Hz; DAMGO 0.60 ± 0.09 Hz; $t_{36} = 5.22$, $P < 0.001$) (Fig. 5*G* and *K*). Additionally, the amplitude of sEPSCs was reduced by 23 ± 5% (control 17.9 ± 1.32 pA; DAMGO 15.46 ± 0.89 pA; $t_{21} = 2.27$, $P < 0.05$) (Fig. 5*G* and *L*).

Effect of MOR activation on miniature PSCs (mPSCs). Following exposure to TTX (1 μM), the resultant mPSCs were also suppressed by DAMGO. The mean frequency of mIPSCs was decreased by 76 ± 9% (control 0.27 ± 0.07 Hz; DAMGO 0.12 ± 0.08 Hz; $t_8 = 2.9$, $P < 0.05$) (Fig. 5*M*). Similarly, the frequency of mEPSCs was reduced by 48 ± 5% (control 1.93 ± 0.54 Hz; DAMGO 1.31 ± 0.46 Hz; $t_{13} = 2.4$, $P < 0.05$) (Fig. 5*O*). Amplitudes of mPSCs were unaffected by DAMGO in the presence of TTX (Fig. 5*N* and *P*).

Melanocortin and MOR agonists attenuates stimulus evoked calcium transients. To further establish the inhibitory nature of α-MSH and DAMGO on activity of Sst-GABA neurons in the DMV, we tested their ability to effect $[Ca^{2+}]_i$ signalling in these neurons. To accomplish this, transgenic mice expressing the Ca^{2+} sensor protein GCaMP3 were crossed with Sst-Cre mice as described previously (Partridge *et al.* 2014). This genetic strategy enabled activation-dependent visualization of Sst-GABA neurons in the DMV.

In brainstem slices, the activity of calcium transients in Sst-GABA DMV neurons evoked by local stimulation was attenuated by 'Y-tube' application of α-MSH (500 nM) (%$\Delta F/F$: baseline 69 ± 14; α-MSH 15 ± 3; $t_6 = 3.4$, $P < 0.05$; $n = 7$) (Fig. 6*A*–*C*). Similarly, as with α-MSH, the MOR agonist DAMGO (1 μM) also robustly attenuated the induced calcium responses in Sst-GABA DMV neurons (%$\Delta F/F$: baseline 94 ± 5, DAMGO 18 ± 11; $t_{10} = 10.98$, $P < 0.0001$; $n = 11$) (Fig. 6*D*–*F*).

Overall, these findings demonstrate that activation of both MC4Rs and MORs inhibits the action potential frequency of Sst-GABA DMV neurons and causes membrane hyperpolarization. Additionally, they show that α-MSH and DAMGO have an inhibitory effect on EPSCs and differential effects on IPSCs, which are increased and decreased respectively. Although changes in these postsynaptic currents may contribute to regulation of the Sst-GABA DMV neurons, this is insufficient to fully explain the suppression of action potential firing in these neurons. Other mechanisms affecting membrane excitability and resting potential may be responsible. For example, in the case of GABAergic neurons in the NTS, exposure to the MOR agonist endomorphin-1 causes hyperpolarization of the membrane that is absent when Cs^+ is substituted in the recording pipette (Glatzer *et al.* 2007). This suggests that activation of MORs hyperpolarizes the membrane by decreasing input resistance through potassium-activated channels. Our current data also show a change in input resistance upon exposure to a MOR agonist. However, this is not the case when Sst-GABA DMV neurons are exposed to the MC4R agonist.

Melanocortin and opioid agonists attenuate Sst-GABA neuron-mediated inhibition of DMV neurons projecting to the gastric-antrum

Because both melanocortin and opioid agonists influenced the neural activity of Sst-GABA neurons in the DMV, we were interested to determine whether the agonists could alter the ability of Sst-GABA neurons to inhibit identified vagal output neurons to the stomach. This would establish that the neurons affected by the above agonists were the same population as those involved in the gastric circuit regulating the antrum. To test the function of Sst-GABA neurons in our circuit, we recorded from antrum projecting DMV neurons monosynaptically labelled with DiI in Sst-GABA-CHR2 transgenic mice. In the neurons tested ($n = 8/8$), optogenetic stimulation with blue light suppressed the activity of gastric-antrum-projecting DMV neurons ($t_7 = 5.4$, $P < 0.001$) (Fig. 7*A* and *B*, left). This light-induced suppression of action potentials was counteracted by bath application of α-MSH (500 nM) such that there was no significant difference between baseline activity (absence of light) and during light stimulation ($n = 3$) (Fig. 7*A* and *C*, right). Voltage clamp recording showed that this effect coincided with a significant decrease in the light-induced IPSCs that are of Sst-GABA neuronal origin ($n = 5$) (Fig. 7*E* and *G*).

Similarly, light-induced inhibition of neural activity in antrum-projecting neurons in the DMV was prevented when they were exposed to the μ-opioid agonist, DAMGO (100 nM; $n = 5$) (Fig. 7*B* and *D*). This was correlated with a significant suppression of the increase in sIPSCs associated with light stimulation ($n = 6$) (Fig. 7*F* and *H*).

G, left: representative voltage clamp recording ($V_H = -30$ mV) showing the change in input resistance after DAMGO exposure. *G*, right: representative voltage clamp recording ($V_H = -30$ mV) showing sPSCs before (top) and during (bottom) exposure to DAMGO. *H*, DAMGO increases in the input resistance of Sst-GABA neurons ($n = 17$, $^{**}P < 0.01$). *I* and *J*, DAMGO decreases sIPSC frequency ($n = 18$; $^{**}P < 0.01$) and amplitude ($n = 13$; $^{**}P < 0.01$) in Sst-GABA neurons. *K* and *L*, DAMGO decreases sEPSC frequency ($n = 24$; $^{***}P < 0.001$) and amplitude ($n = 22$; $^{**}P < 0.01$) of Sst-GABA neurons. *M* and *N*, DAMGO decreases mIPSC frequency ($n = 9$; $^{**}P < 0.01$) but not amplitude ($n = 7$; $P > 0.05$) of Sst-GABA neurons. *O* and *P*, DAMGO decreases mEPSC frequency ($n = 16$; $^{**}P < 0.01$) but not amplitude ($n = 15$; $P > 0.05$) of Sst-GABA neurons.

These studies show that activation of MC4R or MOR receptors in the DMV disrupts local GABA signalling in the DMV. This is reflected in the inability of gastric-coupled Sst-GABA neurons to significantly suppress the activity of vagal neurons in the DMV that innervate the antrum.

Discussion

Focusing on the DMV, our studies have uncovered a key role for Sst-GABA neurons in local GABA signalling that has a robust inhibitory effect on vagal output to the stomach. This is based on our major findings showing that Sst-GABA neurons are: (1) anatomically connected to DMV output neurons that innervate the gastric-antrum; (2) functionally connected to DMV output neurons that innervate the gastric-antrum; and (3) an important source of tonic inhibition of DMV output neurons that innervate the antrum; and also (4) themselves under tonic inhibitory drive and (5) inhibited by agonists of the melanocortin and μ-opioid receptors for which activation is known to increase the activity of DMV output neurons that innervate the antrum.

Sst-GABA neurons in the DMV are anatomically connected to DMV output neurons that innervate the gastric-antrum

To establish the role of Sst-GABA DMV neurons as regulators of vagal efferent activity to the stomach, we first had to confirm their identity and then establish

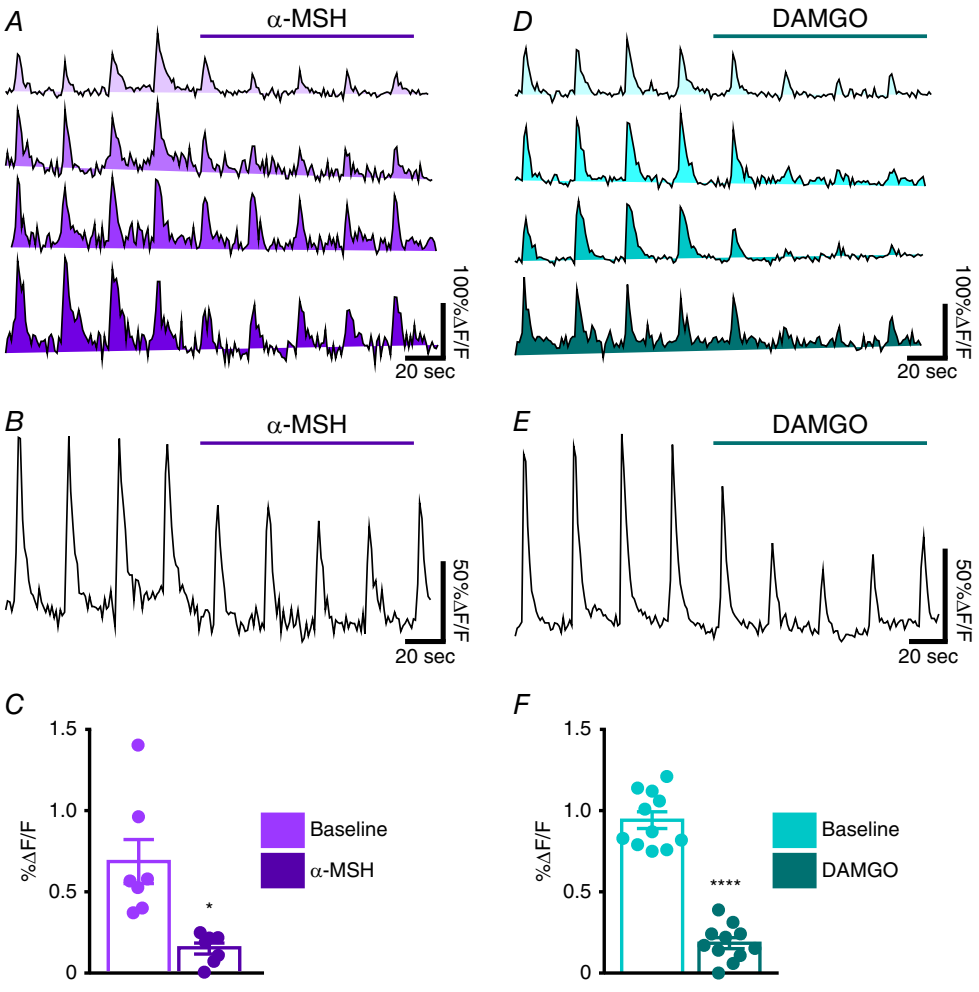

Figure 6. Evoked calcium transients in Sst-GABA neurons in the DMV are attenuated on exposure to MC4R or MOR agonists
A, examples of the time courses of changes in $[Ca^{2+}]$ ($\Delta F/F$) in the region of interest (ROI) corresponding to electrical stimulation of a cell body. *B*, average tracing of all ROIs and (*C*) quantification of the change in response to electrical stimulation in the presence of α-MSH ($n = 7$; $P < 0.05$). *D*, examples of the time courses of changes in $[Ca^{2+}]$ ($\Delta F/F$) in different ROIs and (*E*) average tracing of all ROIs. *F*, quantification of the change in response to electrical stimulation in the presence of DAMGO ($n = 11$; $P < 0.0001$). Each trace represents a distinct ROI or cell body.

whether they were part of the vagal circuitry in the DMV that controls motility. To determine this, we employed electrophysiological cell typing, immunohistochemistry and polysynaptic tract tracing. The Sst-GABA neurons in the DMV exhibited electrophysiological properties similar to those reported for this type of interneurons in the NTS (Wang & Bradley, 2010) and other areas of the brain (Oliva *et al.* 2000; Ma *et al.* 2006; Luo *et al.* 2013). Indeed, in the

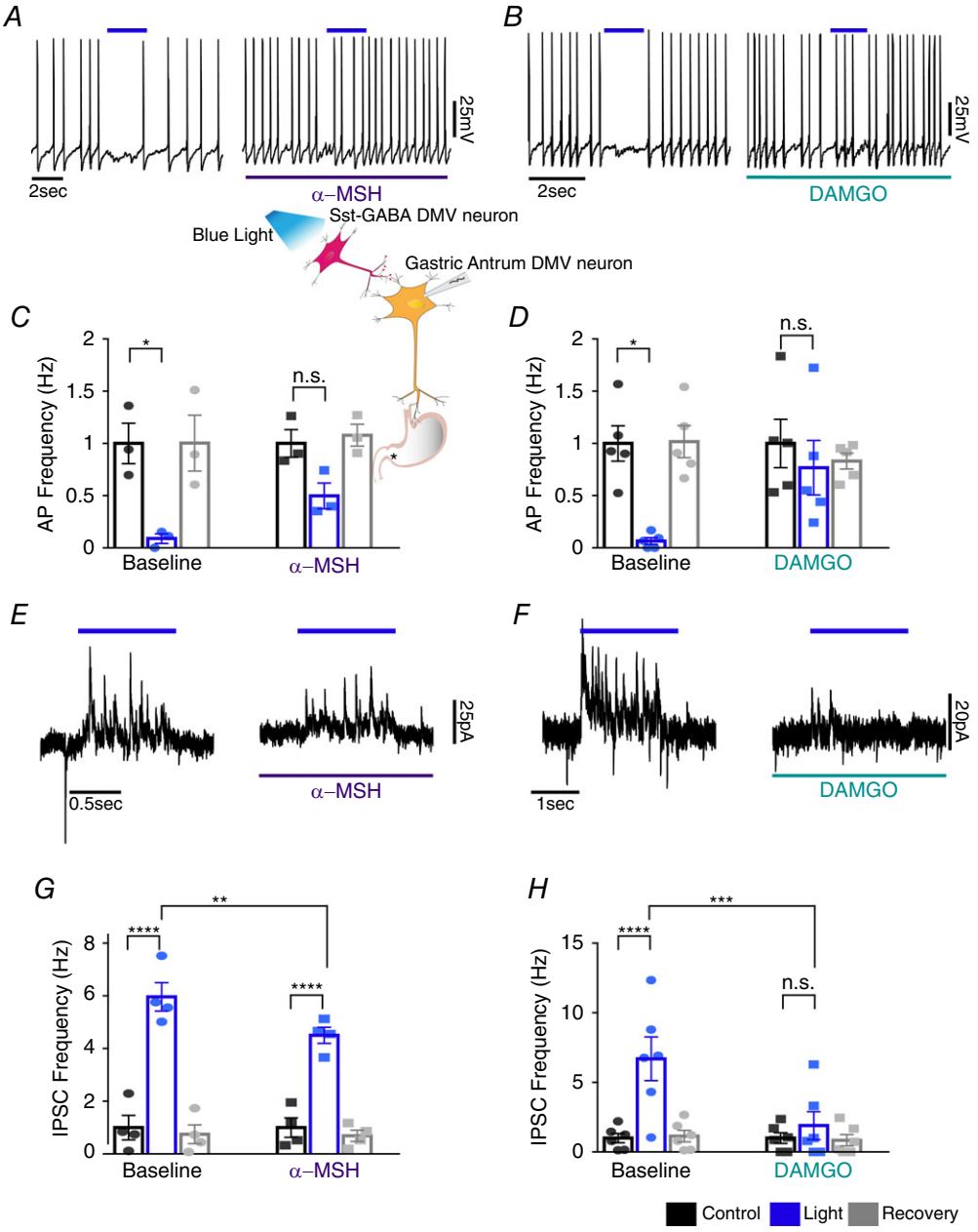

Figure 7. Inhibition of gastric-antrum projecting DMV neurons by Sst-GABA-ChR2-neurons that comprise the gastric circuit is attenuated by MC4R and MOR agonists
A, representative current clamp recording in the absence (left) and presence (right) of α-MSH (500 nM). *B*, representative current clamp recording in the absence (left) and presence (right) of DAMGO (1 μM). *C* and *D*, summary of the effects of α-MSH ($n = 3$; $^{*}P < 0.05$, n.s. $P > 0.05$) and DAMGO ($n = 5$; $^{*}P < 0.05$, n.s. $P > 0.05$) on the light-induced inhibition of action potential frequency in DMV antrum projecting neurons. *E* and *F*, representative voltage clamp recording ($V_H = -30$) showing sPSCs in the absence (left) and presence (right) of α-MSH (*E*) or DAMGO (*F*). *G* and *H*, summary of the effects of α-MSH (*G*, $n = 4$; $^{****}P < 0.0005$, $^{**}P > 0.01$, $^{*}P < 0.05$) and DAMGO (*H*, $n = 6$; $^{****}P < 0.0005$, $^{***}P < 0.001$, $^{**}P < 0.01$, n.s. $P > 0.05$) on the light-induced inhibition of sIPSC frequency in DMV antrum projecting neurons.

cortex of Sst-Cre mice (Hu *et al.* 2013), Cre-mediated recombination has been shown to be prevalent in 92% of Sst-GABA interneurons, although only in 6–10% of parvalbumin positive neurons.

In the present study, 90% of the neurons expressing the Cre-dependent reporter (tdTomato) displayed somatostatin-IR that appeared to be restricted to the perikaryal cytoplasm similar to that seen, for example, in lamina II of the spinal cord (Proudlock *et al.* 1993). Somatostatin-IR in GABA neurons has been reported previously in GAD67-GFP neurons of the rostral NTS in GIN mice (Wang & Bradley, 2010). However, unlike Sst-GABA neurons in the DMV (located at the level of the caudal NTS), only 15% of the GFP neurons were somatostatin positive in the rostral NTS (Wang & Bradley, 2010). However, this may not be reflective of the overall GABAergic population in this area because only 46% of the GABA neurons were GFP positive (Wang & Bradley, 2010). As in the present study, these neurons were observed to be surrounded by fibres that exhibited somatostatin labelling.

To address whether the Sst-GABA neurons were anatomically connected to DMV output neurons projecting to the stomach, we injected the polysynaptic tracer PRV-152 into the gastric-antrum and labelled Sst-GABA neurons in the DMV. The current data indicate that the Sst-GABA neurons in the DMV of our transgenic animals do comprise part of the vagal circuitry that controls motility. These findings corroborate earlier reports of polysynaptic label in a subset of GABAergic neurons in the DMV (Gao *et al.* 2009) when PRV was injected into the stomach.

Our interest in specifically labelling Sst-GABA DMV neurons from the gastric-antrum was based on several considerations. First, this area of the stomach is a major driver of motility (el-Sharkawy *et al.* 1978; Gillis *et al.* 1989; Ludtke *et al.* 1991; Rogers *et al.* 1996), which is under GABAergic control based on data from pharmacological (Sivarao *et al.* 1998; Ferreira *et al.* 2002; Herman *et al.* 2009) and electron microscopy studies (Pearson *et al.* 2011). Second, the distribution of DMV vagal neurons innervating the antrum corresponds well with distribution of MC4Rs and MOR fibres in the nucleus (Mountjoy *et al.* 1994; Martin-Schild *et al.* 1999; Kishi *et al.* 2003; Liu *et al.* 2003).

Sst-GABA neurons are functionally connected to DMV output neurons that innervate the gastric-antrum

In determining the functional connectivity of Sst-GABA neurons to vagal output neurons in the DMV, we optogenetically stimulated or inhibited these neurons at the same time as recording the activity of identified DMV neurons projecting to the gastric-antrum. We found a tight coupling between the excitation of Sst-GABA neurons and inhibition of DMV output neurons innervating the gastric-antrum. Not only did light stimulation distinctly increase the frequency of action potentials in Sst-GABA neurons in the DMV, but also it was accompanied by a simultaneous $GABA_A$-mediated suppression of action potentials in identified DMV neurons, as evident by a considerable increase in IPSCs. Similar targeted activation of Sst-GABA neurons and the resultant inhibition of action potentials in coupled neurons, which is associated with an increase in inhibitory currents, has been reported in other areas of the brain such as the striatum (Nelson *et al.* 2014), entorhinal cortex (Yekhlef *et al.* 2015) and the cerebellum (Najac & Raman, 2015). The ability of Sst-GABA neurons to influence the activity of output neurons to the stomach has important functional implications for gastric motility as it relates to food intake and satiety (Janssen *et al.* 2011). Based on their high basal activity and regulation of network transmission in other brain regions (e.g. in the cortex; Gentet *et al.* 2012; Kvitsiani *et al.* 2013), it is reasonable to speculate that information from the DMV to the stomach is under the tight control of Sst-GABA neurons. Hence, modulation of the activity of these neurons either directly or indirectly would greatly impact gastric activity.

EGFP expressing neurons in the DMV and NTS of GIN mice have been shown to have extensive dendritic ramifications that traverse both nuclei (Gao *et al.* 2009) and to express somatostatin (Wang & Bradley, 2010). Therefore, the source of Sst-GABAergic inhibition to gastric output neurons could potentially originate from the NTS or other nuclei such as the amygdala (Saha *et al.* 2002) and not the DMV. Expression of channelrhodopsin receptors can occur in terminals; hence, their excitation can influence synaptic release at the DMV even though their cell bodies may reside outside the nucleus. However, these fibres have a higher probability of being severed during the slicing process and, although their functional abilities may not be eliminated, they are probably hindered from producing consistent and robust inhibitory effects on output neurons in the DMV.

We propose that the substantial inhibitory input onto DMV output neurons originates primarily from local Sst-GABA neurons in the nucleus and not from those in the NTS. In the present study, light stimulation was restricted primarily to the DMV (Fig. 2) and so both cell bodies and their terminals within the nucleus would be stimulated, thereby producing the strongest rhodopsin-mediated effect on output neurons to the gastric-antrum. Additionally, our *in vivo* studies demonstrate opposite intragastric pressure responses induced by local GABA blockade in the two nuclei (Ferreira *et al.* 2002; Herman *et al.* 2009). Blockade of GABA in the DMV increases gastric motility (Ferreira *et al.* 2002), whereas, in the NTS, it decreases motility (Herman *et al.* 2009). These opposite effects elicited from the DMV and NTS are also observed by microinjection of MC4R or

MOR agonists (Herman *et al.* 2009; Richardson *et al.* 2013). Yet, these same agonists have similar effects on Sst-GABA neurons in the DMV and in the NTS (Lewin A, Vicini S, Gillis RA & Sahibzada N, unpublished data); they are inhibited by both types of agonists. If Sst-GABAergic inhibition on DMV output neurons was of NTS origin, then microinjection of either of these agonists into the NTS would result in an increase in motility because of disinhibition of the DMV gastric-antrum projecting neurons. Instead, both agonists decrease motility when administered into the NTS (Herman *et al.* 2009; Herman *et al.* 2010; Richardson *et al.* 2013), which suggests the presence of two distinct Sst-GABA populations in each nucleus (Fig. 8).

Sst-GABA neurons are an important source of tonic inhibitory drive to DMV output neurons that innervate the gastric-antrum

The distinct presence of baseline inhibitory currents in DMV output neurons to the gastric-antrum led us to investigate whether they received tonic inhibitory drive from Sst-GABA neurons. To establish this, we optogenetically inhibited these neurons. Light inhibition of the Sst-GABA neurons decreased the IPSCs in the DMV neurons projecting to the gastric-antrum, suggesting that they were indeed under tonic inhibition. Regarding whether Sst-GABA neurons are themselves the recipient of inhibitory transmission, our data show that, in the presence of low calcium that would block synaptic transmitter release (Fong & Van der Ploeg, 2000), their firing rate increases. However, these data do not address the source of this inhibition because the data might originate from GABAergic projection neurons in the NTS or from other Sst-GABA neurons. Pair recordings from Sst-GABA neurons in the dentate gyrus of the hippocampus show that Sst-GABA neurons do inhibit one another (Savanthrapadian *et al.* 2014), although this may be specific to the brain region. In the cortex, Sst-GABA neurons, although strongly inhibiting other neurons, do not affect each other (Pfeffer *et al.* 2013).

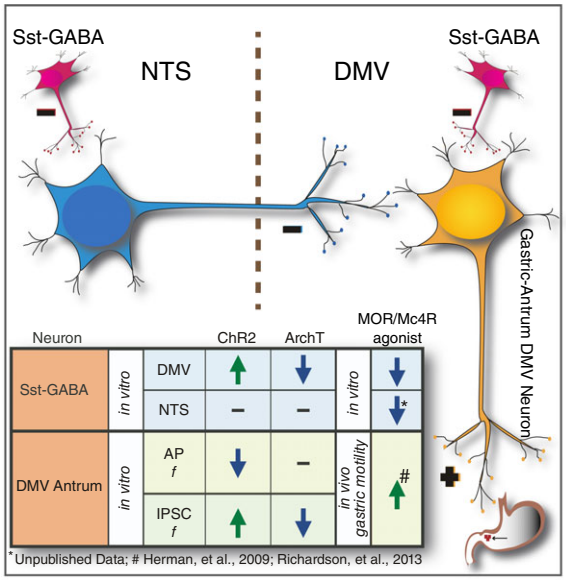

Figure 8. A simple schematic illustrating the relationship of Sst-GABA neurons in the NTS-DMV circuitry that regulates parasympathetic output to the stomach
Both in the DMV and in the NTS, Sst-GABA neurons regulate output signalling whose inhibition by α-MSH or DAMGO results in contrasting effects on motility. This is reminiscent of GABA blockade in both nuclei. In the NTS, inhibition of Sst-GABA neurons 'decouples' inhibitory output (blue neuron) to the DMV that results in suppression of motility. In the DMV, inhibition of Sst-GABA neurons lead to the release of inhibitory 'brake' on excitatory output (orange neuron) to the stomach (i.e. gastric-antrum), which increases motility. The insert summarizes the major findings of the inter-relationship between Sst-GABA neurons and DMV gastric-antrum projecting neurons. AP, action potential; *f*, frequency.

Activation of MC4Rs or MORs inhibits activity of Sst-GABA neurons in the DMV

Exposure of Sst-GABA DMV neurons to agonists of either the MC4R or MOR inhibited their action potentials and hyperpolarized their membrane potential. The MC4R agonist, α-MSH, differentially affected sPSCs in these neurons in a TTX-sensitive manner, such that sIPSCs were increased, whereas sEPSCs were decreased, and mPSCs were unaffected. Similar results for MC4R activation in the DMV have been reported previously for gastric-antrum-projecting output neurons (Richardson *et al.* 2013). However, in these neurons, unlike the Sst-GABA DMV neurons, a postsynaptic excitatory effect was evident when the presynaptic input was blocked (Richardson *et al.* 2013). Direct depolarization of the membrane as a result of MC4R activation by α-MSH has also been reported recently for a subset of NTS neurons (Mimee *et al.* 2014). Additionally, in another subset of NTS neurons, as in the DMV (Richardson *et al.* 2013), α-MSH has also been reported to indirectly enhance sIPSCs and to hyperpolarize the membrane without affecting mIPSCs (Mimee *et al.* 2014). Although it is difficult to determine whether these neurons contribute to the gastric circuit because their identity was unknown, a subset probably comprised of Sst-GABA neurons. In our studies (data not reported), Sst-GABA neurons in the NTS are blocked by α-MSH just as they are in the DMV.

By contrast to the MC4R agonist, exposure to the MOR agonist had a more 'global' effect on Sst-GABA neurons in the DMV. Not only was the frequency and amplitude of sPSCs attenuated, but also the mPSC frequency was suppressed. These observations are in agreement with recordings showing the suppression of GIN neurons in the DMV by the endogenous MOR agonist, endomorphin-1 (Glatzer *et al.* 2007).

Taken together, these findings establish that activation of MC4Rs or MORs inhibits action potential frequency and causes membrane hyperpolarization of Sst-GABA neurons in the DMV. Changes in postsynaptic currents, in conjunction with membrane hyperpolarization and effects on input resistance, offer a potential means by which the Sst-GABA neurons may be regulated by both melanocortin and opioid signalling in the DMV.

MC4R and MOR agonists prevent light-induced suppression of gastric-antrum projecting neurons in the DMV

Optogenetic stimulation of Sst-GABA-ChR2 neurons and the resultant inhibition of action potentials in vagal output neurons to the gastric-antrum were significantly counteracted by both α-MSH and DAMGO. These studies demonstrate that activation of either MC4R or MORs 'decouples' the Sst-GABA neuron from the vagal circuit regulating the gastric-antrum. Hence, by inhibiting Sst-GABA neurons, MC4R and MOR agonists block local GABA, thereby releasing the inhibitory 'brake' posed on projection neurons. This is significant when considering the direct excitatory effect of α-MSH on DMV output neurons (Richardson *et al.* 2013), which could confound the results regarding action potential frequency. However, the accompanying attenuation of light-induced IPSCs by the MC4R agonist with the prevention of action potential frequency inhibition in DMV output neurons argues against this as the primary mechanism.

Our data advance current knowledge about the anatomical and functional connectivity between Sst-GABA neurons and DMV output neurons that innervate the gastric-antrum. Previously, we reported that neurons projecting to the gastric-antrum receive a higher percentage of GABAergic input than neurons projecting to other gastric areas (Pearson *et al.* 2011). Furthermore, GABA blockade at the DMV produces a marked increase in phasic contractions of the stomach (Ferreira *et al.* 2002; Herman *et al.* 2009). These observations, together with data from the present study, suggest that Sst-GABA neurons are an important source of the overwhelming GABAergic drive present at the DMV (and NTS).

In summary, the present study is the first to demonstrate that Sst-GABA neurons are important mediators of the vagal circuitry responsible for motility. As in other areas of the brain, their role most probably extends to shaping network dynamics in an activity-dependent manner. Furthermore, because these neurons are inhibited by the melanocortin and opioid peptides, they represent a target by which other brain areas (e.g. the hypothalamus) homeostatically regulate the vagal circuitry(s) responsible for gastric function.

References

Bailey TW, Appleyard SM, Jin Y-H & Andresen MC (2008). Organization and properties of GABAergic neurons in solitary tract nucleus (NTS). *J Neurophysiol* **99**, 1712–1722.

Cruz MT, Murphy EC, Sahibzada N, Verbalis JG & Gillis RA (2007). A reevaluation of the effects of stimulation of the dorsal motor nucleus of the vagus on gastric motility in the rat. *Am J Physiol Regul Integr Comp Physiol* **292**, R291–R307.

Davis SF, Derbenev AV, Williams KW, Glatzer NR & Smith BN (2004). Excitatory and inhibitory local circuit input to the rat dorsal motor nucleus of the vagus originating from the nucleus tractus solitarius. *Brain Res* **1017**, 208–217.

Drummond GB (2009). Reporting ethical matters in *The Journal of Physiology*: standards and advice. *J Physiol* **587**, 713–719.

el-Sharkawy TY, Morgan KG & Szurszewski JH (1978). Intracellular electrical activity of canine and human gastric smooth muscle. *J Physiol* **279**, 291–307.

Fanselow EE & Connors BW (2010). The Roles of somatostatin-expressing (GIN) and fast-spiking inhibitory interneurons in up-down states of mouse neocortex. *J Neurophysiol* **104**, 596–606.

Fanselow EE, Richardson KA & Connors BW (2008). Selective, state-dependent activation of somatostatin-expressing inhibitory interneurons in mouse neocortex. *J Neurophysiol* **100**, 2640–2652.

Ferreira M, Jr., Sahibzada N, Shi M, Panico W, Niedringhaus M, Wasserman A, Kellar KJ, Verbalis J & Gillis RA (2002). CNS site of action and brainstem circuitry responsible for the intravenous effects of nicotine on gastric tone. *J Neurosci* **22**, 2764–2779.

Fong TM & Van der Ploeg LH (2000). A melanocortin agonist reduces neuronal firing rate in rat hypothalamic slices. *Neurosci Lett* **283**, 5–8.

Gao H, Glatzer NR, Williams KW, Derbenev AV, Liu D & Smith BN (2009). Morphological and electrophysiological features of motor neurons and putative interneurons in the dorsal vagal complex of rats and mice. *Brain Res* **1291**, 40–52.

Gentet LJ, Kremer Y, Taniguchi H, Huang ZJ, Staiger JF & Petersen CC (2012). Unique functional properties of somatostatin-expressing GABAergic neurons in mouse barrel cortex. *Nat Neurosci* **15**, 607–612.

Gillis RA, Quest JA, Pagani FD & Norman WP (1989). Control centers in the central nervous system for regulating gastrointestinal motility. In *Handbook of Physiology The Gastrointestinal System*, eds Schultz SG, Wood JD & Rauner BB, pp. 621–683. The American Physiological Society, Bethesda, MD.

Glatzer N, Hasney C, Bhaskaran M & Smith B (2003). Synaptic and morphologic properties in vitro of premotor rat nucleus tractus solitarius neurons labeled transneuronally from the stomach. *J Comp Neurol* **464**, 525–539.

Glatzer NR, Derbenev AV, Banfield BW & Smith BN (2007). Endomorphin-1 modulates intrinsic inhibition in the dorsal vagal complex. *J Neurophysiol* **98**, 1591–1599.

Halabisky B, Shen F, Huguenard JR & Prince DA (2006). Electrophysiological classification of somatostatin-positive interneurons in mouse sensorimotor cortex. *J Neurophysiol* **96**, 834–845.

Herman MA, Alayan A, Sahibzada N, Bayer B, Verbalis J, Dretchen KL & Gillis RA (2010). micro-Opioid receptor stimulation in the medial subnucleus of the tractus solitarius inhibits gastric tone and motility by reducing local GABA activity. *Am J Physiol Gastrointest Liver Physiol* **299**, G494–G506.

Herman MA, Cruz MT, Sahibzada N, Verbalis J & Gillis RA (2009). GABA signaling in the nucleus tractus solitarius sets the level of activity in dorsal motor nucleus of the vagus cholinergic neurons in the vagovagal circuit. *Am J Physiol Gastrointest Liver Physiol* **296**, G101–G111.

Hu H, Cavendish JZ & Agmon A (2013). Not all that glitters is gold: off-target recombination in the somatostatin-IRES-Cre mouse line labels a subset of fast-spiking interneurons. *Front Neural Circuits* **7**, 195.

Iqbal J, Pompolo S, Dumont LM, Wu CS, Mountjoy KG, Henry BA & Clarke IJ (2001). Long-term alterations in body weight do not affect the expression of melanocortin receptor-3 and -4 mRNA in the ovine hypothalamus. *Neuroscience* **105**, 931–940.

Janssen P, Vanden Berghe P, Verschueren S, Lehmann A, Depoortere I & Tack J (2011). Review article: the role of gastric motility in the control of food intake. *Aliment Pharmacol Ther* **33**, 880–894.

Jarvinen MK & Powley TL (1999). Dorsal motor nucleus of the vagus neurons: a multivariate taxonomy. *J Comp Neurol* **403**, 359–377.

Kishi T, Aschkenasi CJ, Lee CE, Mountjoy KG, Saper CB & Elmquist JK (2003). Expression of melanocortin 4 receptor mRNA in the central nervous system of the rat. *J Comp Neurol* **457**, 213–235.

Kistler-Heer V, Lauber ME & Lichtensteiger W (1998). Different developmental patterns of melanocortin MC3 and MC4 receptor mRNA: predominance of Mc4 in fetal rat nervous system. *J Neuroendocrinol* **10**, 133–146.

Kvitsiani D, Ranade S, Hangya B, Taniguchi H, Huang JZ & Kepecs A (2013). Distinct behavioural and network correlates of two interneuron types in prefrontal cortex. *Nature* **498**, 363–366.

Liu H, Kishi T, Roseberry AG, Cai X, Lee CE, Montez JM, Friedman JM & Elmquist JK (2003). Transgenic mice expressing green fluorescent protein under the control of the melanocortin-4 receptor promoter. *J Neurosci* **23**, 7143–7154.

Ludtke FE, Lammel E, Mandrek K, Peiper HJ & Golenhofen K (1991). Myogenic basis of motility in the pyloric region of human and canine stomachs. *Dig Dis* **9**, 414–431.

Luo R, Janssen MJ, Partridge JG & Vicini S (2013). Direct and GABA-mediated indirect effects of nicotinic ACh receptor agonists on striatal neurones. *J Physiol* **591**, 203–217.

Ma Y, Hu H, Berrebi AS, Mathers PH & Agmon A (2006). Distinct subtypes of somatostatin-containing neocortical interneurons revealed in transgenic mice. *J Neurosci* **26**, 5069–5082.

Markram H, Toledo-Rodriguez M, Wang Y, Gupta A, Silberberg G & Wu C (2004). Interneurons of the neocortical inhibitory system. *Nat Rev Neurosci* **5**, 793–807.

Martin-Schild S, Gerall AA, Kastin AJ & Zadina JE (1999). Differential distribution of endomorphin 1- and endomorphin 2-like immunoreactivities in the CNS of the rodent. *J Comp Neurol* **405**, 450–471.

Mimee A, Kuksis M & Ferguson AV (2014). alpha-MSH exerts direct postsynaptic excitatory effects on NTS neurons and enhances GABAergic signaling in the NTS. *Neuroscience* **262**, 70–82.

Mountjoy KG, Mortrud MT, Low MJ, Simerly RB & Cone RD (1994). Localization of the melanocortin-4 receptor (MC4-R) in neuroendocrine and autonomic control circuits in the brain. *Mol Endocrinol* **8**, 1298–1308.

Najac M & Raman IM (2015). Integration of Purkinje cell inhibition by cerebellar nucleo-olivary neurons. *J Neurosci* **35**, 544–549.

Nelson AB, Hammack N, Yang CF, Shah NM, Seal RP & Kreitzer AC (2014). Striatal cholinergic interneurons drive GABA release from dopamine terminals. *Neuron* **82**, 63–70.

Niedringhaus M, Jackson PG, Pearson R, Shi M, Dretchen K, Gillis RA & Sahibzada N (2008). Brainstem sites controlling the lower esophageal sphincter and crural diaphragm in the ferret: a neuroanatomical study. *Auton Neurosci* **144**, 50–60.

Oliva AA, Jr., Jiang M, Lam T, Smith KL & Swann JW (2000). Novel hippocampal interneuronal subtypes identified using transgenic mice that express green fluorescent protein in GABAergic interneurons. *J Neurosci* **20**, 3354–3368.

Pagani FD, Norman WP, Kasbekar DK & Gillis RA (1985). Localization of sites within dorsal motor nucleus of vagus that affect gastric motility. *Am J Physiol Gastrointest Liver Physiol* **249**, G73–G84.

Partridge JG, Lewin AE, Yasko JR & Vicini S (2014). Contrasting actions of group I metabotropic glutamate receptors in distinct mouse striatal neurones. *J Physiol* **592**, 2721–2733.

Pearson RJ, Gatti PJ, Sahibzada N, Massari VJ & Gillis RA (2007). Ultrastructural evidence for selective noradrenergic innervation of CNS vagal projections to the fundus of the rat. *Auton Neurosci* **136**, 31–42.

Pearson RJ, Gatti PJ, Sahibzada N, Massari VJ & Gillis RA (2011). Ultrastructural evidence for selective GABAergic innervation of CNS vagal projections to the antrum of the rat. *Auton Neurosci* **160**, 21–26.

Pfeffer CK, Xue M, He M, Huang ZJ & Scanziani M (2013). Inhibition of inhibition in visual cortex: the logic of connections between molecularly distinct interneurons. *Nat Neurosci* **16**, 1068–1076.

Proudlock F, Spike RC & Todd AJ (1993). Immunocytochemical study of somatostatin, neurotensin, GABA, and glycine in rat spinal dorsal horn. *J Comp Neurol* **327**, 289–297.

Richardson J, Cruz MT, Majumdar U, Lewin A, Kingsbury KA, Dezfuli G, Vicini S, Verbalis JG, Dretchen KL, Gillis RA & Sahibzada N (2013). Melanocortin signaling in the brainstem influences vagal outflow to the stomach. *J Neurosci* **33**, 13286–13299.

Robinson RB & Siegelbaum SA (2003). Hyperpolarization-activated cation currents: from molecules to physiological function. *Annu Rev Physiol* **65**, 453–480.

Rogers RC, McTigue DM & Hermann GE (1996). Vagal control of digestion: modulation by central neural and peripheral endocrine factors. *Neurosci Biobehav Rev* **20**, 57–66.

Roselli-Rehfuss L, Mountjoy KG, Robbins LS, Mortrud MT, Low MJ, Tatro JB, Entwistle ML, Simerly RB & Cone RD (1993). Identification of a receptor for gamma melanotropin and other proopiomelanocortin peptides in the hypothalamus and limbic system. *Proc Natl Acad Sci USA* **90**, 8856–8860.

Royer S, Zemelman BV, Losonczy A, Kim J, Chance F, Magee JC & Buzsaki G (2012). Control of timing, rate and bursts of hippocampal place cells by dendritic and somatic inhibition. *Nat Neurosci* **15**, 769–775.

Saha S, Henderson Z & Batten TFC (2002). Somatostatin immunoreactivity in axon terminals in rat nucleus tractus solitarii arising from central nucleus of amygdala: coexistence with GABA and postsynaptic expression of sst2A receptor. *J Chem Neuroanat* **24**, 1–13.

Sahibzada N, Ferreira M, Jr., Williams B, Wasserman A, Vicini S & Gillis RA (2002). Nicotinic ACh receptor subtypes on gastrointestinally projecting neurones in the dorsal motor vagal nucleus of the rat. *J Physiol* **545**, 1007–1016.

Savanthrapadian S, Meyer T, Elgueta C, Booker SA, Vida I & Bartos M (2014). Synaptic properties of SOM- and CCK-expressing cells in dentate gyrus interneuron networks. *J Neurosci* **34**, 8197–8209.

Shapiro RE & Miselis RR (1985). The central organization of the vagus nerve innervating the stomach of the rat. *J Comp Neurol* **238**, 473–488.

Sivarao DV, Krowicki ZK & Hornby PJ (1998). Role of $GABA_A$ receptors in rat hindbrain nuclei controlling gastric motor function. *Neurogastroenterol Motil* **10**, 305–313.

Smith BN, Dou P, Barber WD & Dudek FE (1998). Vagally evoked synaptic currents in the immature rat nucleus tractus solitarii in an intact in vitro preparation. *J Physiol* **512**(Pt 1), 149–162.

Taniguchi H, He M, Wu P, Kim S, Paik R, Sugino K, Kvitsani D, Fu Y, Lu J, Lin Y, Miyoshi G, Shima Y, Fishell G, Nelson SB & Huang ZJ (2011). A Resource of Cre Driver Lines for Genetic Targeting of GABAergic Neurons in Cerebral Cortex. *Neuron* **71**, 995–1013.

Travagli RA, Gillis RA, Rossiter CD & Vicini S (1991). Glutamate and GABA-mediated synaptic currents in neurons of the rat dorsal motor nucleus of the vagus. *Am J Physiol Gastrointest Liver Physiol* **260**, G531–G536.

Wang M & Bradley RM (2010). Properties of GABAergic neurons in the rostral solitary tract nucleus in mice. *J Neurophysiol* **103**, 3205–3218.

Yekhlef L, Breschi GL, Lagostena L, Russo G & Taverna S (2015). Selective activation of parvalbumin- or somatostatin-expressing interneurons triggers epileptic seizurelike activity in mouse medial entorhinal cortex. *J Neurophysiol* **113**, 1616–1630.

Additional information

Competing interests

The authors declare that they have no competing interests.

Author contributions

AL, SV, JR, KLD, RAG and NS, conceived and designed the study. AL, SV and NS collected, assembled, analysed and interpreted the data. AL, SV, RAG and NS drafted the manuscript. All studies were completed at Georgetown University Medical Centre. All authors have approved the final version of the manuscript and agree to be accountable for all aspects of the work. All persons designated as authors qualify for authorship, and all those who qualify for authorship are listed.

Funding

This work was supported by NIH Grant RO1 DK57105.

Acknowledgements

We thank Dr Robert C. Switzer III (NeuroScience Associates, Knoxville, TN, USA) for his advice and help with the immunocytochemistry.